

# Supporting Information

## Modulating the Faradic Operation of All-Printed Organic Electrochemical Transistors by Facile in Situ Modification of the Gate Electrode

Matteo Sensi,<sup>†</sup> Marcello Berto,<sup>†</sup> Andrea Candini,<sup>‡</sup> Andrea Liscio,<sup>‡,§</sup> Andrea Cossarizza,<sup>||</sup> Valerio Beni,<sup>⊥</sup> Fabio Biscarini,<sup>†,#</sup> and Carlo Augusto Bortolotti<sup>\*,†</sup>

<sup>†</sup>Dipartimento di Scienze della Vita, Università degli Studi di Modena e Reggio Emilia, Via Campi 103, 41125 Modena, Italy

<sup>‡</sup>Istituto per la Sintesi Organica e la Fotoreattività (ISO-F)-CNR, Via P. Gobetti, 101, 40129 Bologna, Italy

<sup>§</sup>Istituto per la Microelettronica e Microsistemi (CNR-IMM), Via del Fosso del Cavaliere 100, 00133 Roma, Italy

<sup>||</sup>Dipartimento di Scienze Mediche e Chirurgiche Materno-Infantili e dell'Adulto, Università degli Studi di Modena e Reggio Emilia, Via Campi 287, 41125 Modena, Italy

<sup>⊥</sup>Department of Printed Electronics, RISE Acreo, Research Institute of Sweden, Norrköping 164 40, Sweden

<sup>#</sup>Center for Translational Neurophysiology of Speech and Communication, Istituto Italiano di Tecnologia, Via Fossato di Mortara 17-19, 44121 Ferrara, Italy

### Table of contents

<b>1 - Point of zero charge determination</b>	<b>S2</b>
<b>2 - Stability of the OECT in transfer cycles and reproducibility of the data</b>	<b>S2</b>
<b>3 - CV of the Au-C-gate in PBS</b>	<b>S4</b>
<b>4 - Stability of the OECT in ethanol</b>	<b>S4</b>
<b>5 - Drain-source current behaviour during the potential-pulse-assisted deposition of SAMs</b>	<b>S5</b>
<b>6 - Modulation of the current in C-gate devices with different gate area</b>	<b>S6</b>
<b>7 - C-gate OECT use for the electrochemical detection of ascorbic acid</b>	<b>S7</b>

## 1 - Point of zero charge determination

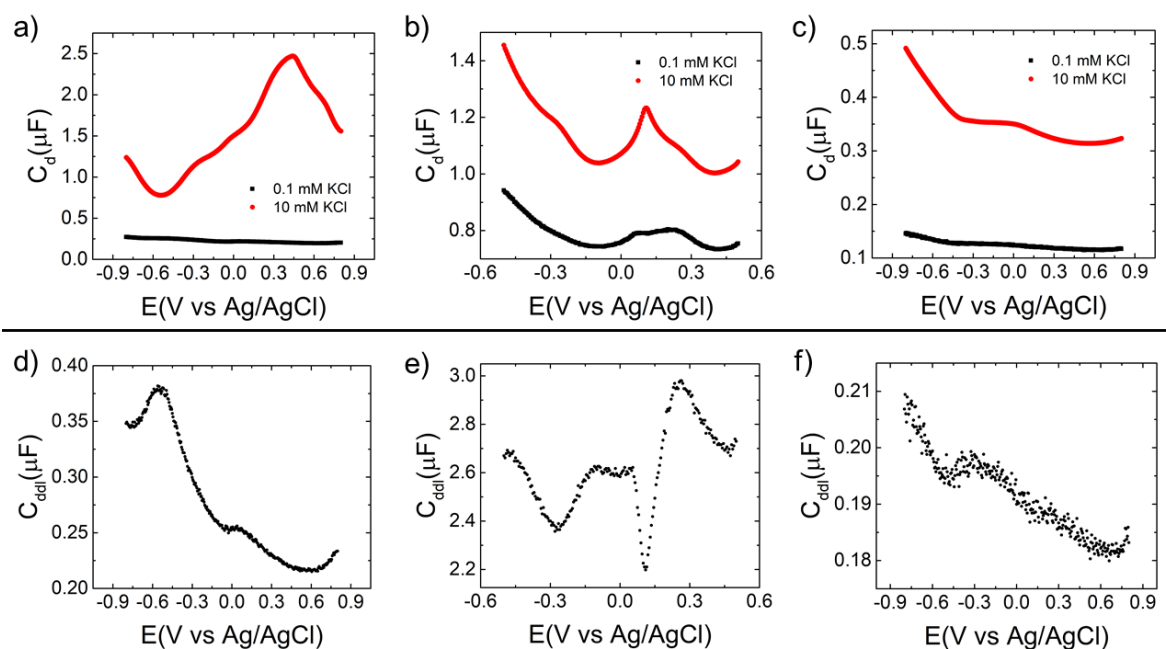


Figure S1 - Determination of the PZC. On top, the  $C_d$  as a function of potential obtained by non-faradic EIS in KCl 0.1 mM (red) or 10 mM (black) for a) Au-C-gate OECT and after functionalization with b) MUA or c) OEG. Below are reported the  $C_{dbl}$  values, as a function of potential, of d) Au-C-gate OECT and after functionalization with e) MUA or f) OEG. The EIS measurements were performed in KCl (0.1 or 1 mM KCl), in an electrochemical cell with a platinum counter electrode, and Ag/AgCl reference electrode and the gate of the OECT connected as working electrode. The frequency was fixed at 100 Hz.

By applying the procedure reported in reference 1, we determined the PZC of the Au-C-gate electrode before and after deposition at open circuit potential (OCP) of the two different SAMs, by performing non-faradic electrochemical impedance spectroscopy (EIS) measurements at fixed frequency (see Fig. S1). The PZC of gold was 0.56 V vs Ag/AgCl, in line with previous findings,<sup>1</sup> while the SAM induced a shift in the PZC potential,<sup>2</sup> which was 0.11 V for MUA and 0.65 V for OEG.

## 2 - Stability of the OECT in transfer cycles and reproducibility of the data

Both the signal of C-gate and Au-C-gate need an initial stabilization step by performing transfer cycles, as observed before, see ref. <sup>3</sup>. As shown in figure S2, once stabilized, the devices can be used for 6 hours with a stable signal (red curve in figure S2, panel a and b) and the signal is stable also after storage in the air for two days (green line in figure S2, panel a and b).

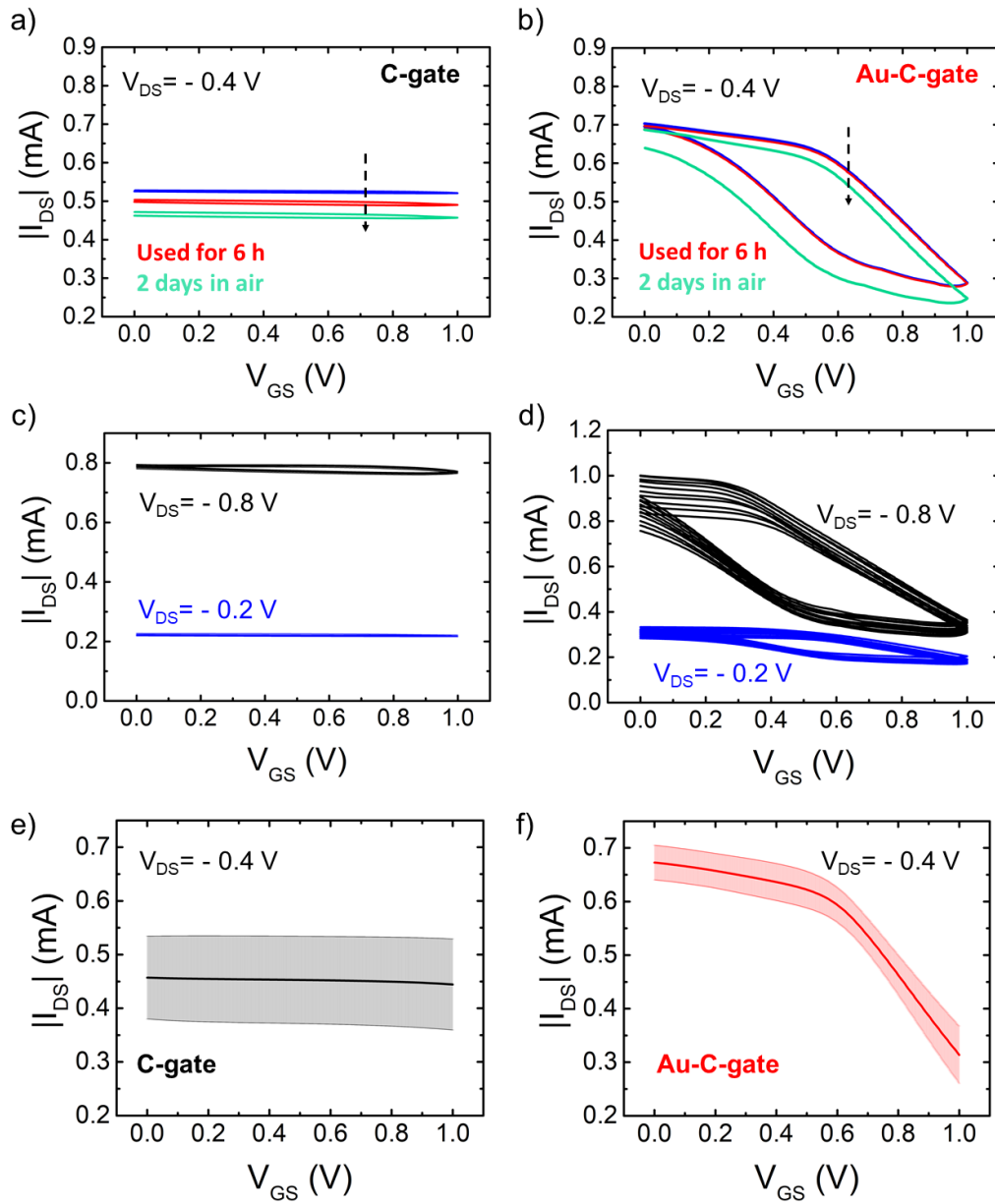


Figure S2 – Reproducibility and stability of the OECT signal. Transfer curves of a single a) C-gate and a single b) Au-C-gate OECTs in PBS 50 mM (pH 7.4),  $V_{DS} = -0.4$  V. The blue curve is the transfer characteristics of the pristine device, the red curves is the transfer curve of the device after it had been operated continuously for 6 hours. The green curve is the transfer curve recorded after a 2-day long storage in air.

Overlay of 8 consecutive transfer curves recorded for a c) C-gate and d) Au-C-gate device at varying source-drain potential values. Blue:  $V_{DS} = -0.2$  V; black:  $V_{DS} = -0.8$  V.

e) and f): Solid lines are the average transfer curves for 8 distinct C-gate and Au-C-gate devices, respectively ( $V_{DS} = -0.4$  V). Error bars represent the standard deviation.

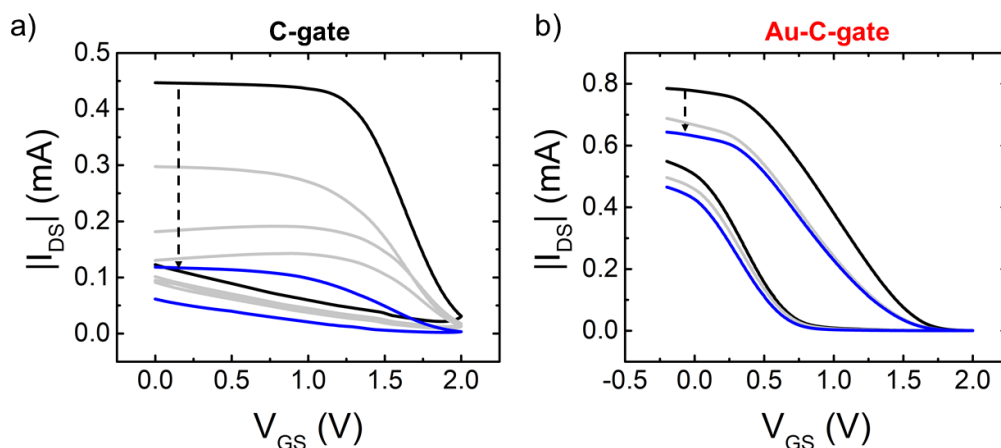


Figure S3 – Hysteresis of the OECT after transfer cycles at high  $V_{GS}$ . Successive transfer curves of a single a) C-gate and a single b) Au-C-gate OECTs in PBS 50 mM,  $V_{DS} = -0.4$  V. The first transfer recorded, in black, has been measured after stabilization at lower  $V_{GS}$ . In blue we show the last transfer cycle measured.

### 3 - CV of the Au-C-gate in PBS

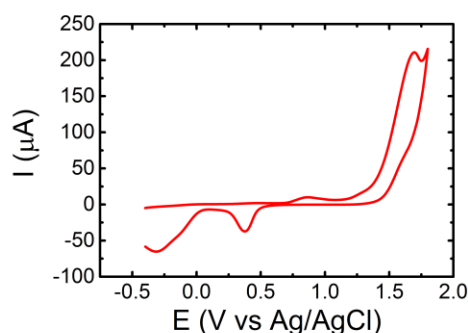


Figure S4 – CV of Au-C-Gate OECTs in PBS. We connected the gate as working electrode and we measured the current vs an Ag/AgCl reference electrode, in presence of a Pt counter electrode, in PBS 50 mM (pH 7.4). We can observe redox peaks that are comparable with the ones observed in the gate current in transfer curves.

### 4 - Stability of the OECT in ethanol

We verified the stability of the Au-C-OECTs by incubating the channel and the gate in a 1:1 water and ethanol solution (the same used to functionalize with the MUA, but without the alkanethiol) overnight, after the characterization of the transfer characteristics ( $V_{GS}$  between 0 V and 1 V;  $V_{DS} = -0.4$  V) in PBS 50 mM. Then, the device was tested again in PBS 50 mM and the transfer curves did not show any significant difference, in terms of overall  $I_{DS}$  and shape of the curve, compared with the curves measured before the incubation, as shown in figure S1.

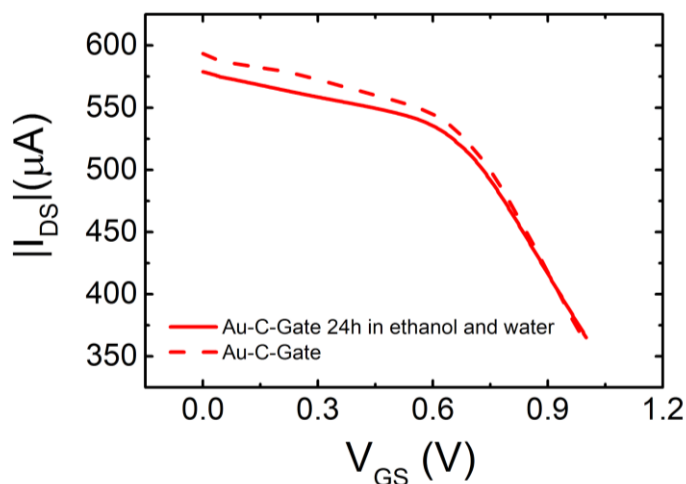


Figure S5 - Stability of the Au-C-Gate OECTs in ethanol and water. Transfer curves recorded in PBS 50 mM pH 7.4 with  $V_{DS} = -0.4$  V before (dashed line) and after (solid line) incubation of the device in an ethanol and water solution overnight.

## 5 - Drain-source current behaviour during the potential-pulse-assisted deposition of SAMs

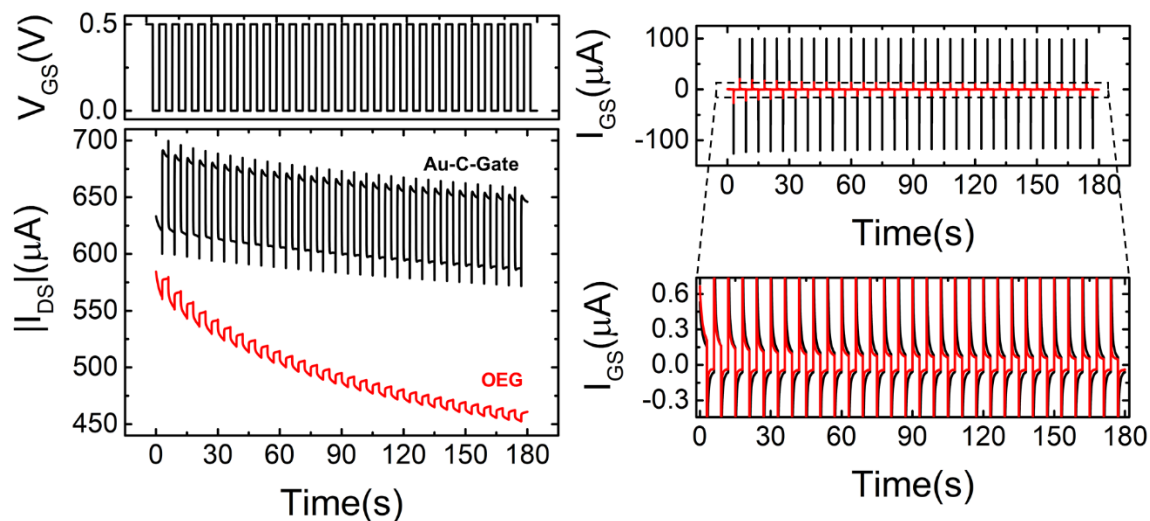


Figure S6 - Profile of  $I_{DS}$  (Left) and  $I_{GS}$  (right) during the potential-pulse-assisted functionalization of Au-C-gate with OEG. On left is reported the applied  $V_{GS}$  against time and below the  $I_{DS}$  as a function of time of the Au-C-gate pulsed in PBS 50 mM (black trace) and the Au-C-gate pulsed in PBS 50 mM with OEG 0.1 mM (red trace).

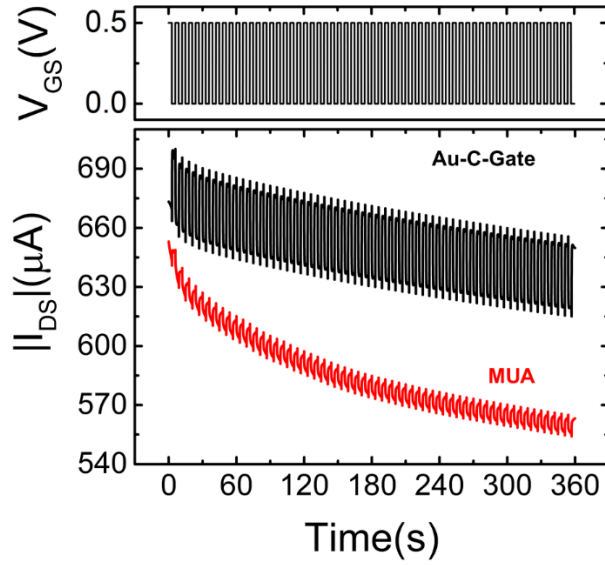


Figure S7 - Profile of  $I_{DS}$  during the potential-pulse-assisted functionalization of Au-C-gate with MUA. Both measurements were performed in a 1:1 water/ethanol mixture, with (red) or without (black) MUA (1 mM).

## 6 – Modulation of the current in C-gate devices with different gate area

We evaluated the influence of the gate dimension on the electrical properties of the C-gate device in 50 mM PBS by characterizing C-gate OECTs with three different nominal gate to channel area ratio, namely:  $A_{gate}:A_{channel} = 0.5, 1$  and  $2$ . To facilitate the comparison between the different devices, we plot the relative variation of the current  $\Delta I = I_x - I_{max}$ , where  $I_x$  is the drain current  $I_{DS}$  at a given  $V_{GS}$  value, and  $I_{max}$  is  $I_{DS}$  at  $V_{GS} = 0V$ . The electrical response is slightly affected by the variation in the gate area, with the modulation for devices featuring the larger gate starting at lower (less positive)  $V_{GS}$ .

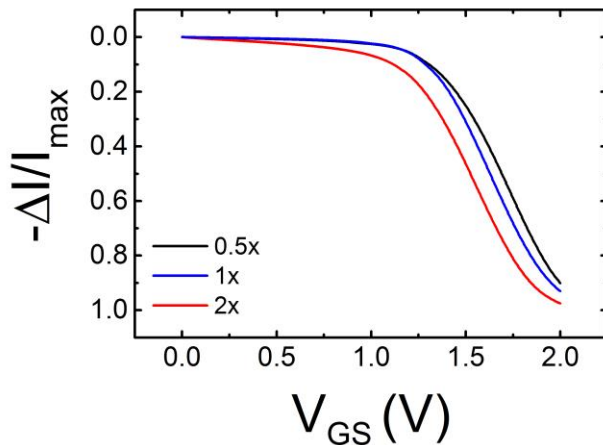


Figure S8 –  $\Delta I/I_{max}$  vs  $V_{GS}$  for C-gate devices with  $A_{gate}:A_{channel} = 0.5$  (black),  $1$  (blue) and  $2$  (red) in 50 mM PBS,  $V_{DS} = -0.4V$ .

## 7 – C-gate OECT use for the electrochemical detection of ascorbic acid

We show here a simple example of application of the C-gate devices. In the following figure is shown the detection of Ascorbic Acid (AA) in PBS 50 mM solution by oxidation. As shown in panel a), when  $V_{GS} > -0.1$  V the AA (2 mM) is oxidized, which is clear from the increase of gate current (gray) compared to the measurement performed without ascorbic acid. Because of the faradic process, the channel current is modulated and the device is turned off at 1 V, instead of 2 V. We also show in panel c) and d) that we observed the same change in the  $I_{DS}$  and  $I_{GS}$  as a function of time, at  $V_{GS} = 0.3$  V and  $V_{DS} = -0.4$  V, injecting PBS solutions with different AA concentrations (0.5, 1 and 2 mM) and then washing with PBS.

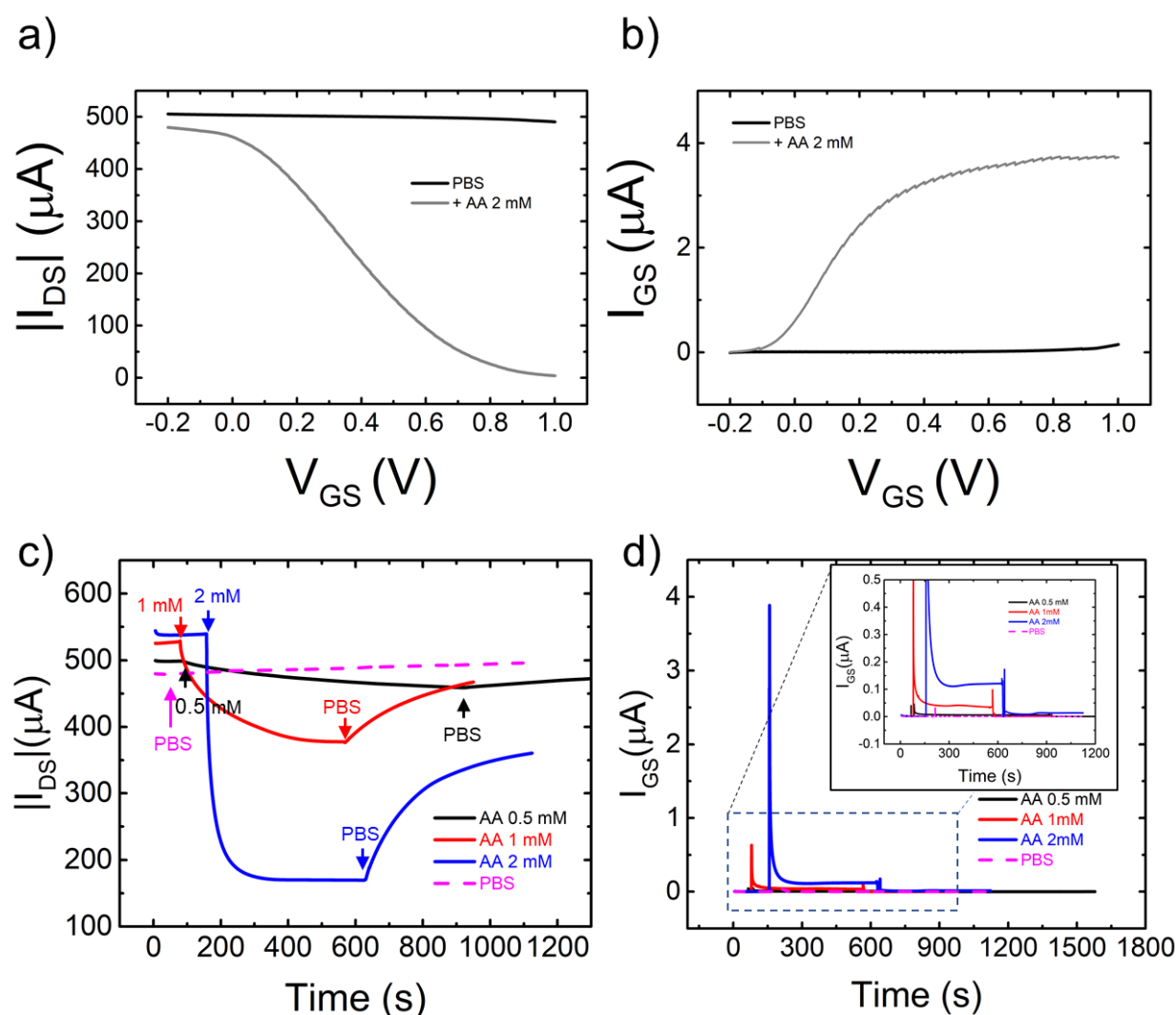


Figure S9 – Detection of Ascorbic Acid by a C-gate OECT. a) Gate and b) channel current of the C-gate OECT in PBS 50 mM (black) and in PBS 50 mM with 2 mM Ascorbic Acid (gray). c)  $I_{DS}$  and d)  $I_{GS}$  as a function of time of a C-gate device in PBS, after changing the solution with PBS (control experiment, in magenta), 0.5 mM AA (black), 1 mM AA (red) and 2 mM AA (blue). After stabilization of the signal the solution was removed and the PDMS pool was filled with PBS (50 mM, pH 7.4). The measurements were performed at  $V_{GS} = 0.3$  V and  $V_{DS} = -0.4$  V.

## References

- (1) Jambrec, D.; Gebala, M.; La Mantia, F.; Schuhmann, W. Potential-Assisted DNA Immobilization as a Prerequisite for Fast and Controlled Formation of DNA Monolayers. *Angew. Chemie - Int. Ed.* **2015**, *54* (50), 15064–15068.
- (2) Kuznetsov, V.; Papastavrou, G. Ion Adsorption on Modified Electrodes as Determined by Direct Force Measurements under Potentiostatic Control. *J. Phys. Chem. C* **2014**, *118* (5), 2673–2685.
- (3) Stavriniidou, E.; Leleux, P.; Rajaona, H.; Khodagholy, D.; Rivnay, J.; Lindau, M.; Sanaur, S.; Malliaras, G. G. Direct Measurement of Ion Mobility in a Conducting Polymer. *Adv. Mater.* **2013**, *25* (32), 4488–4493.